

# Auxin Is Rapidly Induced by Herbivore Attack and Regulates a Subset of Systemic, Jasmonate-Dependent Defenses<sup>1</sup>[OPEN]

Ricardo A.R. Machado, Christelle A.M. Robert, Carla C.M. Arce, Abigail P. Ferrieri, Shuqing Xu, Guillermo H. Jimenez-Aleman, Ian T. Baldwin, and Matthias Erb\*

Max Planck Institute for Chemical Ecology, 07745 Jena, Germany (R.A.R.M., C.A.M.R., C.C.M.A., A.P.F., S.X., G.H.J.-A., I.T.B., M.E.); Institute of Plant Sciences, University of Bern, 3013 Bern, Switzerland (R.A.R.M., C.A.M.R., C.C.M.A., M.E.); and Departamento de Entomologia, Universidade Federal de Viçosa, 36570-000 Viçosa, Brazil (C.C.M.A.)

ORCID IDs: 0000-0001-7010-4604 (S.X.); 0000-0001-5371-2974 (I.T.B.); 0000-0002-4446-9834 (M.E.).

Plant responses to herbivore attack are regulated by phytohormonal networks. To date, the role of the auxin indole-3-acetic acid (IAA) in this context is not well understood. We quantified and manipulated the spatiotemporal patterns of IAA accumulation in herbivore-attacked *Nicotiana attenuata* plants to unravel its role in the regulation of plant secondary metabolism. We found that IAA is strongly, rapidly, and specifically induced by herbivore attack. IAA is elicited by herbivore oral secretions and fatty acid conjugate elicitors and is accompanied by a rapid transcriptional increase of auxin biosynthetic YUCCA-like genes. IAA accumulation starts 30 to 60 s after local induction and peaks within 5 min after induction, thereby preceding the jasmonate (JA) burst. IAA accumulation does not require JA signaling and spreads rapidly from the wound site to systemic tissues. Complementation and transport inhibition experiments reveal that IAA is required for the herbivore-specific, JA-dependent accumulation of anthocyanins and phenolamides in the stems. In contrast, IAA does not affect the accumulation of nicotine or 7-hydroxygeranylinalool diterpene glycosides in the same tissue. Taken together, our results uncover IAA as a rapid and specific signal that regulates a subset of systemic, JA-dependent secondary metabolites in herbivore-attacked plants.

Plants withstand herbivore attack by specifically recognizing the attacker and mounting appropriate defenses. Induced defense responses are activated by hormone-mediated signaling cascades (Erb et al., 2012; Wu and Baldwin, 2009), and jasmonates (JAs) have emerged as key regulators in this context (De Geyter et al., 2012; Howe and Jander, 2008). As a consequence,

their behavior and mode of action have been studied in great detail (Wasternack and Hause, 2013). Similarly, other stress-related hormones such as salicylic acid, abscisic acid, and ethylene have been shown to play important roles in the orchestration of plant defenses against herbivores (von Dahl et al., 2007; Winz and Baldwin, 2001; Thaler and Bostock, 2004; Zhang et al., 2013; Kroes et al., 2015). Recent evidence also suggests that hormones that have traditionally been classified as growth regulators participate in induced defense responses. Cytokinins for instance modulate wound-induced local and systemic defense responses (Schäfer et al., 2015), and gibberellins are involved in regulating the plant's investment into growth and defense (Li et al., 2015; Hou et al., 2010; Yang et al., 2012).

In contrast to the hormones mentioned above, little is known about the role of auxins in induced responses against herbivores. Auxins regulate a vast array of plant processes including growth and development as well as responses to light, gravity, abiotic stress, and pathogen attack (Glick, 2015; Mano and Nemoto, 2012; Yang et al., 2014). Several studies suggest that the auxin indole-3-acetic acid (IAA) also regulates gall formation, since some gall-forming herbivores contain high levels of IAA (Mapes and Davies, 2001a, 2001b; Tooker and de Moraes, 2011a; Straka et al., 2010; Dorchin et al., 2009; Yamaguchi et al., 2012; Tanaka et al., 2013), IAA pools and signaling are enhanced

<sup>1</sup> This work was supported by the Max Planck Society, by a Humboldt Postdoctoral Research Fellowship (A.P.F.), by the Brazilian National Council for Research CNPq (grant no. 237929/2012-0 to C.C.M.A.), by Marie Curie Intra European Fellowships (grant no. 328935 to S.X. and grant no. 273107 to M.E.), by the Swiss National Foundation Fellowship (grant nos. 140196 to C.A.M.R. and 134930 to M.E.), by the European Research Council (grant no. 293926 to I.T.B.), and by the Human Frontier Science Program (grant no. RGP0002/2012 to I.T.B.).

\* Address correspondence to matthias.erb@ips.unibe.ch.

The author responsible for distribution of materials integral to the findings presented in this article in accordance with the policy described in the Instructions for Authors ([www.plantphysiol.org](http://www.plantphysiol.org)) is: Ian T. Baldwin ([baldwin@ice.mpg.de](mailto:baldwin@ice.mpg.de)).

R.A.R.M., M.E., and I.T.B. designed the research; R.A.R.M., C.C.M.A., A.P.F., C.A.M.R., G.H.J.-A., and S.X. carried out the experiments; R.A.R.M., M.E., and I.T.B. analyzed data; R.A.R.M. and M.E. wrote the first draft of the article; M.E., R.A.R.M., I.T.B., A.P.F., C.C.M.A., G.H.J.-A., S.X., and C.A.M.R. revised the article; all authors read and approved the final manuscript.

[OPEN] Articles can be viewed without a subscription.

[www.plantphysiol.org/cgi/doi/10.1104/pp.16.00940](http://www.plantphysiol.org/cgi/doi/10.1104/pp.16.00940)

in parasitized plant tissue (Yamaguchi et al., 2012; Tooker and de Moraes, 2011b), and direct application of IAA can result in the formation of gall-resembling structures (Hamner and Kraus, 1937; Guiscafrearrillaga, 1949; Schaller, 1968; Bartlett and Connor, 2014; Connor et al., 2012). In the context of chewing insects, however, our understanding is more limited (Dafae et al., 2013). IAA levels seem to remain unaltered in goldenrod (*Solidago altissima*) and wheat (*Triticum aestivum*) attacked by *Heliothis virescens* caterpillars (Tooker and de Moraes, 2011a, 2011b) and to be reduced in *Helicoverpa zea* attacked maize (*Zea mays*; Schmelz et al., 2003) and *Manduca sexta*-challenged *Nicotiana attenuata* leaves (Onkokesung et al., 2010; Woldemariam et al., 2012). Moreover, mechanical wounding alone can either increase or decrease IAA levels in the leaves (Thornburg and Li, 1991; Tanaka and Uritani, 1979; Machado et al., 2013). A limitation of some of these early studies is that IAA was measured at single time points or during the later stages of infestation (Onkokesung et al., 2010; Schmelz et al., 2003; Tooker and de Moraes, 2011a, 2011b), which may have resulted in an incomplete picture of IAA dynamics under herbivore attack. We recently demonstrated in *N. attenuata* that IAA is induced in locally damaged leaves upon simulated *M. sexta* attack (Machado et al., 2013).

IAA signaling may influence plant responses to herbivore attack by modulating other hormonal pathways and defenses (Erb et al., 2012). For instance, exogenous IAA reduces the herbivory-induced accumulation of nicotine and jasmonates (Baldwin et al., 1997; Baldwin, 1989), gene expression of jasmonate-dependent proteinase inhibitors genes (Kernan and Thornburg, 1989), and vegetative storage proteins (DeWald et al., 1994; Liu et al., 2005). Conversely, IAA promotes the production of phenolics and flavonoids in root cell cultures in a dose-dependent manner (Lulu et al., 2015; Mahdieh et al., 2015) and the auxin homolog 2,4-dichlorophenoxyacetic acid acts as a strong inducer of defense responses in rice (*Oryza sativa*; Xin et al., 2012; Song, 2014).

In this study, we aimed to understand the spatio-temporal patterns of IAA accumulation in herbivore-attacked *N. attenuata* plants as well as the role of IAA in regulating the biosynthesis of secondary metabolites. In an earlier study, we found that IAA accumulates within 1 h following the application of *M. sexta* oral secretions to wounded leaves. To understand this pattern in more detail, we first evaluated IAA accumulation dynamics in several plant organs in response to real and simulated *M. sexta* attack, including the application of a specific herbivore elicitor to wounded leaves, at different time points ranging from 15 s to 6 h. Second, we analyzed the induction of potential IAA biosynthetic genes. Finally, we manipulated IAA accumulation and transport as well as jasmonate signaling to unravel the impact of *M. sexta*-induced IAA on systemic, jasmonate-dependent secondary metabolites. Our experiments reveal that IAA is a rapid herbivory-induced

signal that acts in concert with jasmonates to regulate the systemic induction of plant secondary metabolites.

## RESULTS

### Real and Simulated *M. sexta* Attack Induces the Accumulation of IAA in the Leaves

To investigate the behavior of IAA in herbivore-attacked plants, we measured IAA concentrations in the leaves of *N. attenuata* subjected to either real or simulated *M. sexta* attack (Fig. 1, A–D). We observed a significant increase in IAA levels in response to real *M. sexta* herbivory 3 h after infestation. This effect could be mimicked by leaf wounding and simultaneous application of either *M. sexta* oral secretions (W+OS) or the fatty acid-amino acid conjugate *N*-linolenoyl-Glu as a specific herbivore elicitor (W+FAC; Fig. 1, A–D). Wounding alone led to a delayed and weaker increase in IAA (Fig. 1C). The herbivory-induced accumulation of IAA started 30 to 60 s after induction (Fig. 1B) and occurred independently of the time of day at which the induction took place (Supplemental Fig. S1). Overall, IAA concentrations increased 2- to 3-fold in herbivore induced leaves compared to controls.

### IAA Induction Gradually Spreads through the Shoots of Attacked Plants

To explore whether IAA also increases in systemic tissues, we induced *N. attenuata* plants and measured IAA concentrations in local, treated plant tissues and systemic, untreated plant tissues at different time points over a 2-h time period. Again, we found a rapid increase in IAA levels locally upon simulated *M. sexta* attack (W+OS), which transiently and steadily spread to systemic, untreated tissues (Fig. 2, A–F). IAA levels slightly increased in petioles 10 min after treatment, in stems 60 min after treatment, and in systemic leaves 120 min after treatment. No significant changes were found in the main and lateral roots (Fig. 2, A–F).

### IAA Induction in Leaves Is Conserved across Different Developmental Stages

Herbivore-induced jasmonate and ethylene signaling are influenced by plant development (Diezel et al., 2011a). To test whether plant development specifically influences *M. sexta*-induced IAA levels, we induced plants by simulated *M. sexta* attack and measured IAA levels in the leaves of early rosette, elongated, and flowering plants. We found that the herbivore-elicited increase in IAA concentration was independent of plant developmental stage (Fig. 3, A–C). However, the absolute IAA levels and magnitude of induction were strongest in early rosette plants (Fig. 3, A–C).

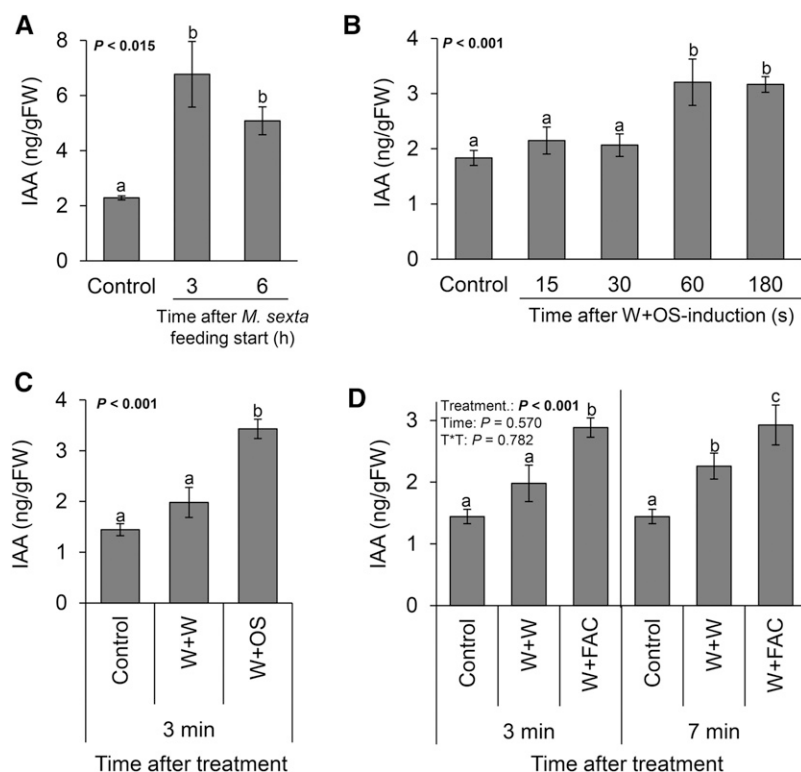


**Figure 1.** IAA is induced specifically and rapidly by real and simulated *M. sexta* attack. Average ( $\pm$ SE) IAA levels in leaves that are attacked by *M. sexta* caterpillars (A), treated with *M. sexta* oral secretions (B and C), or treated with an herbivore elicitor (D;  $n = 5$ ). Different letters indicate significant differences between treatments ( $P < 0.05$ ). Control, intact plants; W+W, wounded and water-treated plants; W+OS, wounded and *M. sexta* oral secretion-treated plants; W+FACs, wounded and fatty acid-amino acid conjugate-treated plants.

### YUCCA-Like, IAA Biosynthesis Homologs Are Rapidly Up-Regulated upon Herbivore Attack

In *Arabidopsis* (*Arabidopsis thaliana*), YUCCA genes encode for flavin monooxygenase-like proteins that convert indole-3-pyruvic acid into IAA, a reaction that likely represents the rate-limiting step in IAA biosynthesis (Mashiguchi et al., 2011; Fig. 4A). We identified YUCCA-like genes in *N. attenuata* and measured their transcript levels upon herbivore elicitation. To achieve this, we first searched the sequence of the *Arabidopsis* YUCCA2 gene (NCBI accession number NM\_117399.3) in the *N. attenuata* draft genome (Ling et al., 2015) and reconstructed the phylogenetic tree of the gene family (Mashiguchi et al., 2011). Our analysis revealed that the *N. attenuata* genome contains at least nine YUCCA-like genes that share high similarity with *AtYUCCA2* and contain the four conserved amino acid motifs characteristic of this gene family (Supplemental Fig. S2; Expósito-Rodríguez et al., 2007, 2011). We designed specific primers and profiled the expression patterns of these genes upon simulated *M. sexta* attack. Several YUCCA-like genes were upregulated in response to simulated *M. sexta* attack (Fig. 4, B–I). *NaYUCCA-like 1, 3, 5, 6, and 9* were upregulated 3 min after the application of *M. sexta* oral secretions and fatty acid-conjugates (Fig. 4, B–H). The up-regulation of *NaYUCCA-like 1* and *3* was maintained for at least one hour (Fig. 4, G and H). The expression of *NaYUCCA-like 2, 4, 7, and 8* was not significantly influenced by simulated *M. sexta* attack (Supplemental Fig. S3).

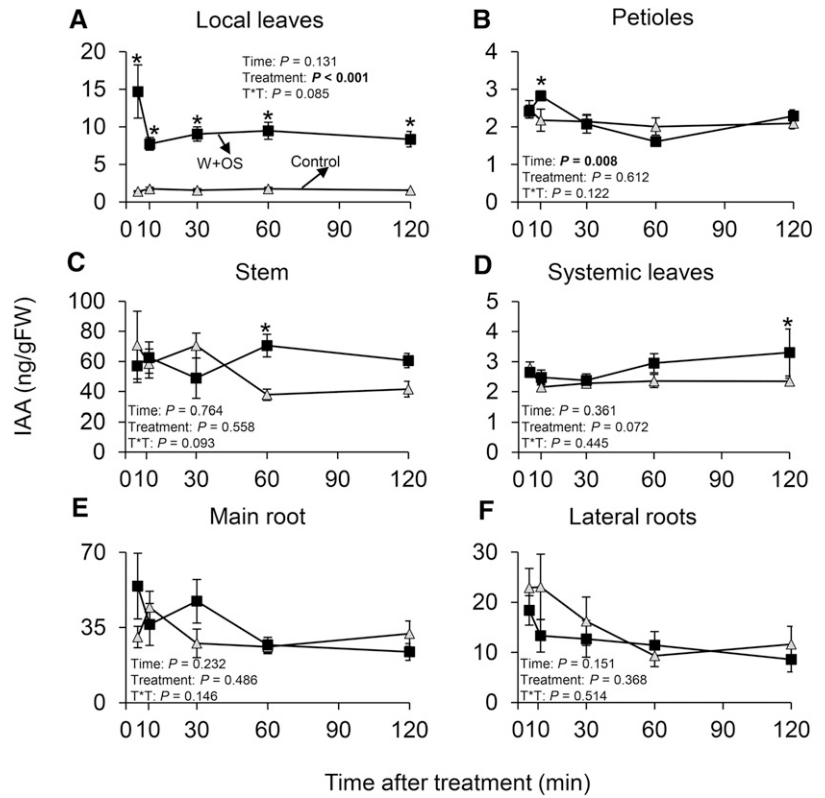
### IAA Accumulation Precedes the JA Burst

To investigate the temporal dynamics of IAA and JA accumulation in *M. sexta*-attacked plants, we quantified IAA and JA in plants subjected to simulated *M. sexta* herbivory at different time points. We found that IAA peaked more rapidly than jasmonic acid in response to herbivore attack (Fig. 5). IAA accumulation commenced within minutes after the onset of the elicitation and reached its maximum 5 min after induction. JA accumulated in an equally rapid fashion, but peaked significantly later than IAA (Fig. 5).

### JA Signaling Is Not Required for the *M. sexta*-Induced IAA Accumulation

Plant responses to attackers are modulated by a complex signaling network consisting of antagonistic, neutral, and synergistic effects (Erb et al., 2012). For example, jasmonate signaling antagonizes IAA signaling (Chen et al., 2011). To further explore the potential crosstalk between these two phytohormones, we measured *M. sexta*-induced IAA in transgenic plants that are impaired to different degrees in jasmonate signaling, biosynthesis, and/or perception (Table I). We found that the *M. sexta*-triggered accumulation of IAA does not require JA signaling as it was induced in all of the evaluated JA-deficient genotypes (Fig. 6; Supplemental Fig. S4).

**Figure 2.** Herbivory induces IAA both locally and systemically. Average ( $\pm$ SE) IAA levels following simulated *M. sexta* attack in local, treated leaves (A) and in untreated petioles (B), stem (C), systemic leaves (D), main root (E), and lateral roots (F;  $n = 5$ ). Asterisks indicate significant differences between treatments within plant tissues and time points ( $*P < 0.05$ ;  $***P < 0.001$ ). Control, intact plants; W+OS, wounded and *M. sexta* oral secretion-treated plants.

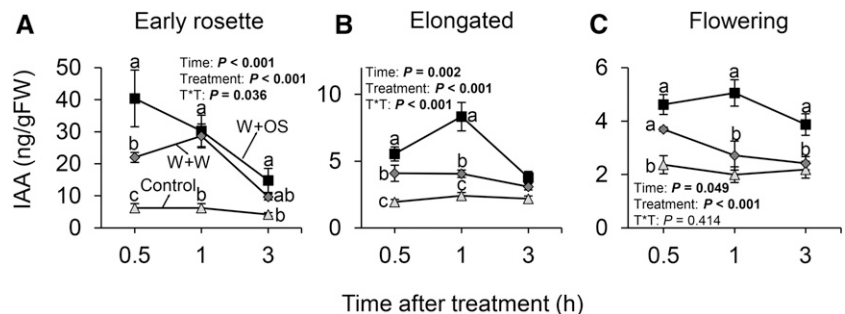


***M. sexta*-Induced IAA Is Required for the Induction of Anthocyanins in the Stems**

To investigate the impact of IAA on plant secondary metabolites, we sought to manipulate its perception in planta. Our initial attempts to create transgenic, dexamethasone-inducible plants (Schäfer et al., 2013) harboring a silencing construct for the IAA receptor TIR1 failed, either because of promoter methylation in the F2 crosses (Weinhold et al., 2013) or because the identified TIR1 homolog was inactive. We therefore took advantage of our knowledge on systemic IAA accumulation to devise a series of chemical manipulation experiments. First, we exogenously applied IAA and methyl jasmonic acid (MeJA) at doses that exceed endogenous levels (Baldwin, 1989; Machado et al., 2013). Second, we inhibited local IAA synthesis with L-kynurenine (L-Kyn). L-Kyn is a specific inhibitor of

Trp aminotransferases, which are key enzymes of the indole-3-pyruvic acid pathway that leads to IAA formation (He et al., 2011). Third, we inhibited IAA transport at the leaf base and petiole of the induced leaves using 2,3,5-triiodobenzoic acid (TIBA). TIBA inhibits auxin polar transport by blocking auxin efflux transporter PIN-FORMED1 cycling (Geldner et al., 2001). We observed that within hours following *M. sexta* attack, *N. attenuata* stems became red (Fig. 7D, inset), a phenotype that is likely due to anthocyanin accumulation. As IAA can regulate the production of anthocyanins in plants (Pasqua et al., 2005), we quantitatively and qualitatively evaluated anthocyanin accumulation in the stems following several simulated and real herbivory treatments in combination with IAA manipulation. We observed that the levels of anthocyanins in the stems were strongly induced by real *M. sexta* attack, an effect that could be mimicked by

**Figure 3.** IAA induction in leaves occurs across different developmental stages. Average ( $\pm$ SE) IAA levels in local treated leaves following simulated *M. sexta* attack at the early rosette (A), elongated (B), and flowering stage (C;  $n = 5$ ). Different letters indicate significant differences between treatments within developmental stages and time points ( $P < 0.05$ ). Control, intact plants; W+W, wounded and water-treated plants; W+OS, wounded and *M. sexta* oral secretion-treated plants.



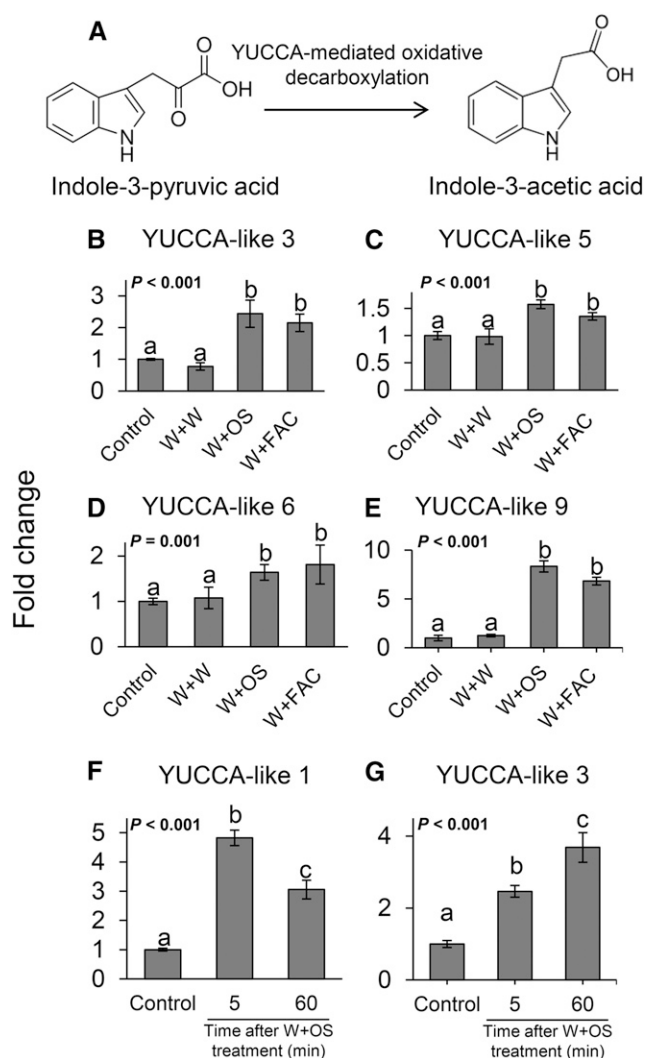


**Figure 4.** YUCCA-like genes are upregulated in response to simulated *M. sexta* herbivory. A, Schematic representation of YUCCA-mediated conversion of indole-3-pyruvic acid into IAA. Average ( $\pm$ SE) transcript abundance relative to control of YUCCA-like 3 (B), YUCCA-like 5 (C), YUCCA-like 6 (D), and YUCCA-like 9 (E) in treated leaves three minutes after elicitation, and YUCCA-like 1 (F) and YUCCA-like 3 (G) 5 and 60 min following simulated *M. sexta* attack ( $n = 3$ ). Different letters indicate significant differences between treatments ( $P < 0.05$ ). Control, intact plants; W+W, wounded and water-treated plants; W+OS, wounded and *M. sexta* oral secretion-treated plants; W+FACs, wounded and fatty acid-amino acid conjugate-treated plants.

wounding and applications of *M. sexta* oral secretions (W+OS), but not by wounding alone (W+W; Fig. 7A). Application of IAA or MeJA alone did not trigger anthocyanin accumulation (Fig. 7A). By contrast, the simultaneous application of IAA and MeJA (IAA+MeJA) triggered anthocyanin accumulation (Fig. 7A). Chemical inhibition of IAA biosynthesis or transport as well as genetic inhibition of JA biosynthesis led to the complete disappearance of induced anthocyanin accumulation (Fig. 7, B and C). Furthermore, we found a positive

correlation between anthocyanin contents and red pigmentation in the stems (Fig. 7D).

### IAA Specifically Potentiates the Herbivore-Induced Accumulation of Phenolamides in the Stems

To investigate the role of IAA in the accumulation of known defensive metabolites in the stems of *N. attenuata* (Onkokesung et al., 2012; Heiling et al., 2010; Paschold et al., 2007), we induced leaves of *N. attenuata* plants by different simulated and real herbivory treatments and complemented them with IAA at doses that exceed endogenous levels (Baldwin, 1989; Machado et al., 2013). The stems of *N. attenuata* are often attacked by herbivores, including stem borers (Diezel et al., 2011b; Lee et al., 2016), and are very important for plant fitness (Machado et al., 2016). We observed a strong up-regulation of defensive secondary metabolites in the stems in response to *M. sexta* attack (Fig. 8, A–D). Petiole pretreatments with IAA dramatically increased the accumulation of caffeoylputrescine and dicaffeoylspermidine in response to real and simulated herbivory as well as MeJA application. IAA application alone did not induce these metabolites (Fig. 8, A and B). By contrast, nicotine and 7-hydroxygeranylinalool diterpene glycosides did not respond to IAA petiole pretreatments (Fig. 8, A–D).

### DISCUSSION

In this study, we show that auxin is a rapidly and specifically induced regulator of defensive secondary

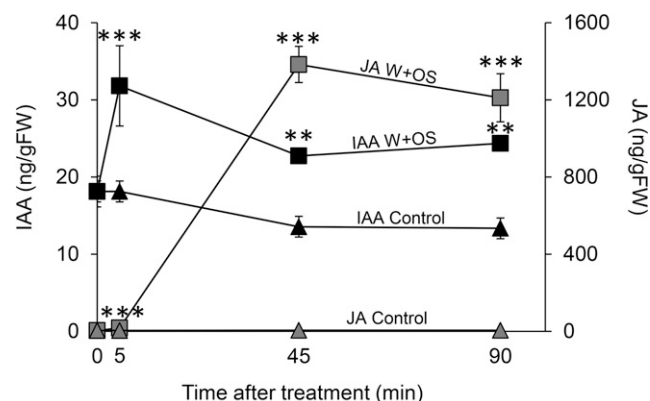


**Figure 5.** *M. sexta*-induced IAA peaks earlier than JA. Left y axis, average ( $\pm$ SE) leaf IAA levels in response to *M. sexta* attack; right y axis, average ( $\pm$ SE) leaf JA levels in response to *M. sexta* attack. Closed squares, IAA levels upon W+OS treatments; closed triangles, IAA levels in control, untreated plants; gray squares, JA levels upon W+OS treatments; gray triangles, JA levels in control, untreated plants ( $n = 5$ ). Asterisks indicate significant differences between treatments for individual metabolites ( $P < 0.05$ ). IAA: time,  $P = 0.015$ ; treatment,  $P < 0.001$ ; time\* treatment,  $P = 0.638$ . JA: time,  $P < 0.001$ ; treatment,  $P < 0.001$ ; time\* treatment,  $P < 0.001$ . Control: intact plants; W+OS, wounded and *M. sexta* oral secretion-treated plants.

**Table 1.** Characteristics of the inverted repeat transgenic lines used in this study

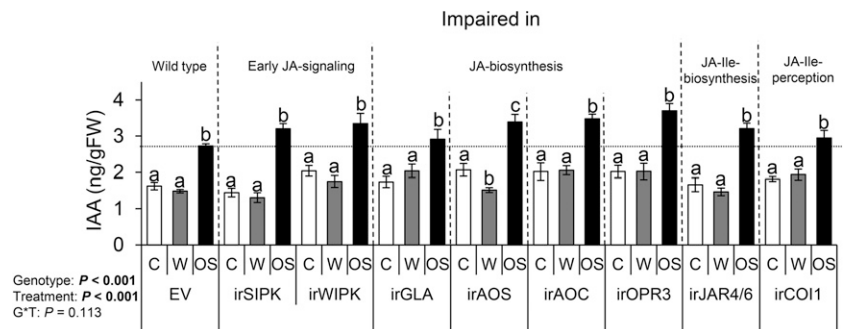
Genotype	Gene Silenced/Overexpressed	Impaired Function	Phenotype	Reference
irSIPK	Salicylic acid-induced mitogen activated protein kinase	Early JA signaling	Reduced levels of JAs	Meldau et al. (2009)
irWIPK	Wound-induced mitogen activated protein kinase	Early JA signaling	Reduced levels of JAs	Meldau et al. (2009)
irGLA1	Glycerolipase A1	JA biosynthesis	Reduced levels of JAs	Bonaventure et al. (2011)
irAOS	Allene oxide synthase	JA biosynthesis	Reduced levels of JAs	Kallenbach et al. (2012)
irAOC	Allene oxide cyclase	JA biosynthesis	Reduced levels of JAs	Kallenbach et al. (2012)
irOPR3	12-Oxo-phytodienoic acid reductase	JA biosynthesis	Reduced levels of JAs	Kallenbach et al. (2012)
irJAR4/6	JA-Ile synthetase	JA-Ile perception	Reduced levels of JA-Ile	Wang et al. (2008)
irCOI1	Coronatine-insensitive 1	JA-Ile perception	Reduced JA-Ile perception	Paschold et al. (2007)

metabolites in *N. attenuata*. Infestation by *M. sexta* caterpillars induced the accumulation of IAA levels in local tissues, an effect that could be mimicked by both the applications of *M. sexta* oral secretions and the application of the well known insect elicitor *N*-linolenoyl-Glu (Halitschke et al., 2003), and to a lesser extent by mechanical wounding. These results are in contrast to earlier studies in maize, goldenrod, and *N. attenuata*, which showed either a slight decrease or no changes in IAA levels in response to herbivore attack (Schmelz et al., 2003; Tooker and de Moraes, 2011a, 2011b; Onkokesung et al., 2010), but are in agreement with our previous study (Machado et al., 2013). Interestingly, in comparison with our previous study, we observed differences in both absolute quantities and timing of IAA induction. One possible explanation for these differences is that plants were grown using different substrates. While sand was used in the previous study, potting soil was used in this article. Given the strong feedback effects of soil bacteria, soil nutrients, and root growth on IAA signaling (Lambrecht et al., 2000; Kurepin et al., 2015; Tian et al., 2008; Sassi et al., 2012), it is likely that the growth substrate affected IAA homeostasis and responsiveness in *N. attenuata*. On the other hand, the absence of IAA induction reported in earlier studies may be due to the fact that late time points were measured (Onkokesung et al., 2010; Schmelz et al., 2003; Tooker and de Moraes, 2011a), which may not have captured the rapid and dynamic accumulation of IAA following herbivore attack. To further investigate these contradicting results, we determined IAA responses in herbivore attacked maize

plants (Maag et al., 2016). We found that IAA levels increased in an herbivore-specific manner 1 to 6 h after the onset of the attack. Together, these experiments suggest that the rapid and transient herbivory-induced accumulation of IAA may be a conserved plant response to insect attack.

Spatiotemporal IAA profiling revealed that the rapid increase in IAA pools at the site of attack is followed by a weak and transient increase in auxin pools in systemic tissues. Similar to what has been observed for other phytohormones (Koo et al., 2009; Stitz et al., 2011; VanDoorn et al., 2011), IAA levels increased sequentially in petioles, stems, and systemic leaves. Together with the rapid local induction of YUCCA-like IAA biosynthetic homologs and the absence of IAA-dependent systemic defense induction in transport inhibitor treated plants, these data suggest that IAA might be synthesized de novo at the site of the attack and then transported across the plant. Several studies have demonstrated that auxin is a mobile signal in plants (Reed et al., 1998; Bhalerao et al., 2002; Jin et al., 2015; van Noorden et al., 2006). Based on the IAA accumulation kinetics, we estimate that herbivory-induced IAA would need to be transported at a speed of at least  $0.29 \text{ cm} \cdot \text{min}^{-1}$  to reach the petioles 5 to 10 min after elicitation (based on the fact that IAA accumulates locally 30 to 60 s after elicitation). This value is at least 10-fold greater than typical values of polar auxin transport velocities (Kramer et al., 2011), but 20-fold slower than wound-induced electrical signals that trigger systemic JA accumulation (Mousavi et al., 2013). We propose two hypotheses that may be

**Figure 6.** Jasmonate signaling is not required for the *M. sexta*-induced accumulation of IAA. A. Average ( $\pm$ se) IAA levels in local, treated leaves of wild-type plants (empty vector [EV]) and plant genotypes impaired in early JA signaling, jasmonate biosynthesis, and/or JA-Ile perception 45 min after elicitation ( $n = 5$ ). Different letters indicate significant differences between treatments within each genotype ( $P < 0.05$ ). C, control, intact plants; W, wounded and water-treated plants; OS, wounded and *M. sexta* oral secretion-treated plants.



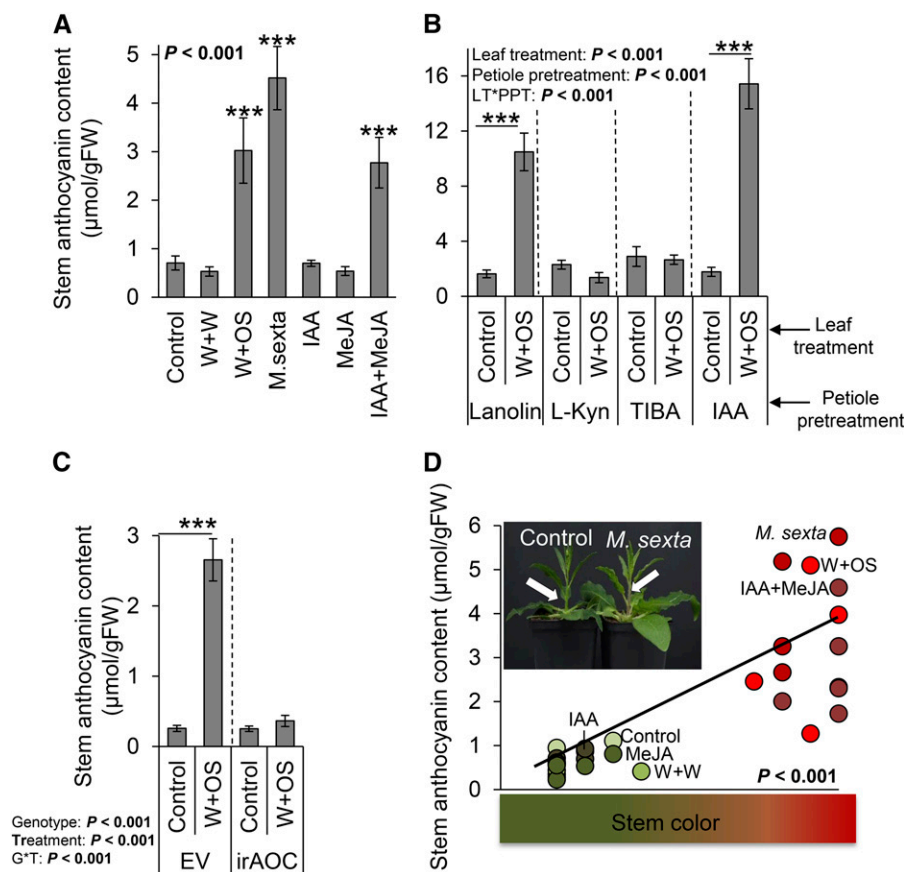


**Figure 7.** *M. sexta*-induced IAA and JA act synergistically to trigger anthocyanin accumulation in the stems. A, Average ( $\pm$ SE) stem anthocyanin content 5 d following either simulated or continuous *M. sexta* attack, exogenous application of MeJA, and/or IAA ( $n = 5$ ). B, Average ( $\pm$ SE) stem anthocyanin content 5 d following simulated *M. sexta* attack and petiole pretreatments with either IAA, the IAA biosynthesis inhibitor L-Kyn, or the IAA transport inhibitor TIBA ( $n = 12$ ). C, Average ( $\pm$ SE) stem anthocyanin contents following simulated *M. sexta* attack of wild-type and JA-impaired *irAOC* plants ( $n = 10$ ). D, Correlation between stem anthocyanin content and stem coloration. Inset: Photograph of the red stem phenotype. Asterisks indicate significant differences between treatments and control (A), between simulated herbivory treatments within petiole pretreatments (B), and between treatments within genotypes (C; \* $P < 0.05$ ; \*\* $P < 0.01$ ; \*\*\* $P < 0.001$ ). The correlation between stem coloration index and stem anthocyanin content was evaluated by a Pearson product moment test. Leaf treatments were as follows: control, intact plants; W+W, wounded and water-treated plants; W+OS, wounded and *M. sexta* oral secretion-treated plants; *M. sexta*, plants subjected to actual *M. sexta* attack; IAA, rosette leaves treated with IAA; MeJA, rosette leaves treated with MeJA; IAA+MeJA, rosette leaves treated with IAA and MeJA. Petioles were treated with either pure lanoline paste, L-Kyn, TIBA, or IAA dissolved in lanoline 1 h prior to leaf treatments.

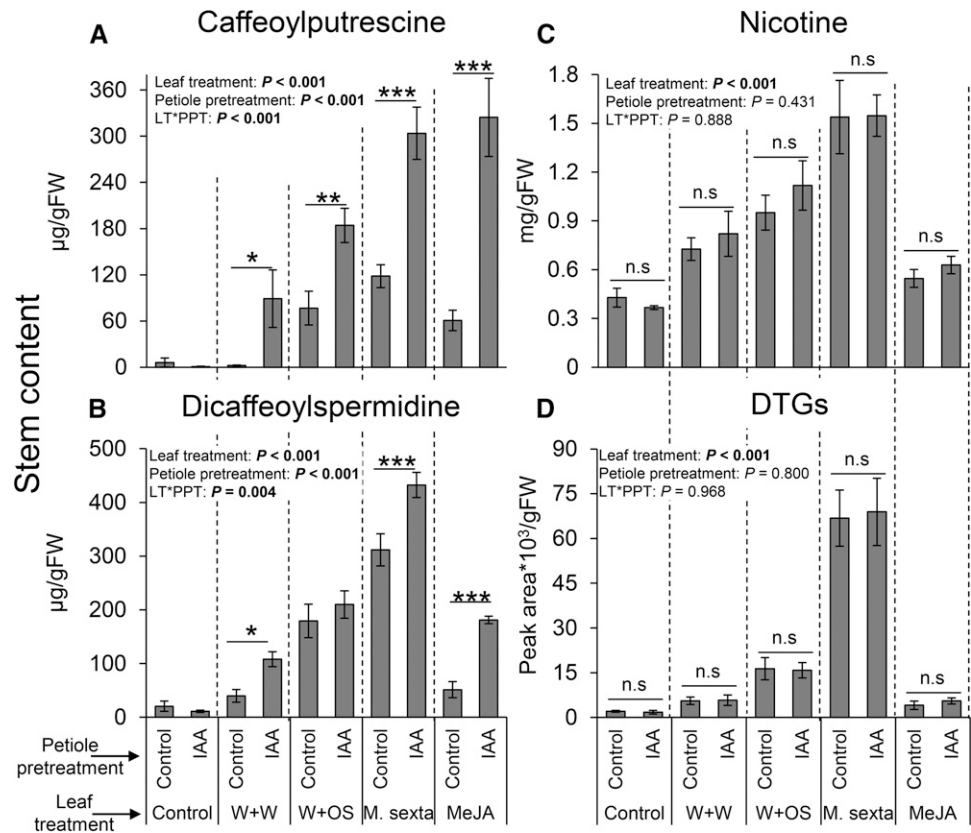
responsible for the atypical signal propagation speed that we observed. First, it is possible that IAA is transported to systemic tissues by a combination of both polar and nonpolar, phloem-based transport (Friml, 2003). Second, rapid secondary signals, including electrical potentials, may spread through the plant at high speeds and induce de novo IAA biosynthesis in systemic tissues. Further experiments with IAA radiotracers (Agtuca et al., 2014) and transient, tissue-specific deactivation of IAA biosynthesis (Koo et al., 2009) would help to shed further light on the exact mechanisms responsible for the systemic spread of IAA following herbivore attack.

Impairing key genes of the jasmonate signaling cascade including mitogen-activated protein kinases,

jasmonate biosynthesis, and jasmonate perception elements did not impair the herbivory-induced accumulation of IAA, suggesting that IAA induction does not require JA signaling. This observation is consistent with the temporal dynamics of herbivory-induced IAA and JA that we observed. IAA accumulation peaks within 5 min after the onset of the elicitation while JA starts accumulating in an equally rapid fashion, but peaks significantly later than IAA (Fig. 5).

An important aim of our study was to understand whether IAA is involved in the regulation of induced secondary metabolites in *N. attenuata*. Because of the systemic accumulation pattern of IAA and the possibility to block this effect through the local application of transport inhibitors, we chose to focus on the induction

**Figure 8.** IAA specifically potentiates the herbivore-induced, systemic production of phenolamides. Average ( $\pm$ SE) caffeoylputrescine (A), dicaffeoylspermidine (B), nicotine (C), and diterpene glycoside (D) levels in the stems 5 d following simulated or real *M. sexta* attack and petiole pretreatments with IAA ( $n = 5$ ). Asterisks indicate significant differences between petiole pretreatments within simulated *M. sexta* attack treatments (\* $P < 0.05$ ; \*\* $P < 0.01$ ; \*\*\* $P < 0.001$ ). Petiole pretreatments were as follows: control, petioles treated with pure lanoline paste 1 h prior to leaf treatments; IAA, petioles treated with IAA dissolved in lanoline 1 h prior to leaf treatments. Leaf treatments were as follows: control, intact plants; W+W, wounded and water-treated plants; W+OS, wounded and *M. sexta* oral secretion-treated plants; *M. sexta*, plants subjected to actual *M. sexta* attack; MeJA, rosette leaves treated with MeJA dissolved in lanoline paste.



of stem secondary metabolites. The stem of *N. attenuata* is vital for its reproduction and can be attacked by a wide variety of organisms, including vertebrates and invertebrate stem borers (Machado et al., 2016; Diezel et al., 2011b). We observed that real and simulated *M. sexta* attack induced anthocyanin accumulation in the stems, an effect that could not be reproduced by MeJA or IAA treatments alone, but by the combination of these two hormones. Together with the IAA transport and biosynthesis inhibitor treatments and the genetic silencing of JA biosynthesis, all of which led to the disappearance of the anthocyanin response, these results strongly suggest that IAA is required to activate the JA-dependent accumulation of stem anthocyanins. In *Arabidopsis*, anthocyanin production is controlled by the MYB75 transcription factor Production of Anthocyanin Pigment 1 (Shin et al., 2015; Borevitz et al., 2000), which is transcriptionally upregulated by IAA (Lewis et al., 2011), and posttranscriptionally repressed by jasmonate-ZIM-domain proteins (Qi et al., 2011). The resulting coregulation of MYB transcription factors by IAA and JA provides a potential mechanism for the synergistic interaction between JA and IAA observed in our study.

In a second set of experiments, we found that IAA also boosts the production of phenolamides in herbivore-attacked plants. Phenolamide accumulation in *N. attenuata* is controlled by the transcription factor MYB8 in a JA-dependent manner (Onkokesung et al.,

2012; Paschold et al., 2007). This transcription factor may therefore represent a target for the integration of IAA and JA signaling. While IAA strongly potentiated the accumulation of stem phenolamides, it had little effect on the accumulation of other JA-dependent secondary metabolites, including nicotine and 7-hydroxygeranylinalool diterpene glycosides (Machado et al., 2013, 2016; Paschold et al., 2007; Jimenez-Aleman et al., 2015). This result is consistent with earlier studies showing neutral to negative effects of auxin application on nicotine accumulation in *Nicotiana* spp. (Baldwin, 1989; Baldwin et al., 1997; Shi et al., 2006). The direct application of IAA to wounded tissues can even suppress local damage-induced JA accumulation (Von Dahl and Baldwin, 2004; Baldwin et al., 1997; Shi et al., 2006). From these results, it is evident that IAA does not simply enhance JA signaling but that it specifically modulates a plant's defensive network. Thereby, IAA signaling may help plants to mount specific, fine-tuned responses to different attackers.

The ecological function of an up-regulation of anthocyanin and phenolamide compounds in the stems upon *M. sexta* attack remains an open question. However, the current literature provides interesting insights in this context. *Trichobaris* stem weevils prefer to feed and perform better on defenseless, jasmonate-deficient plants in a species-specific manner: *T. compacta* grows better on nicotine-impaired *N. attenuata* plants, while *T. mucorea* is not affected by nicotine but by other, yet

unknown, jasmonate-dependent defenses (Diezel et al., 2011b; Lee et al., 2016). It is therefore possible that the IAA-triggered potentiation of jasmonate-dependent secondary metabolite accumulation in the stems may reduce the performance of stem feeders. To disentangle the specific effects that IAA signaling has in this context requires the development of IAA signaling-impaired genotypes and represents an interesting prospect of this study.

In conclusion, this study identifies IAA as a rapid and specific signal that regulates a biologically relevant subset of herbivory-induced secondary metabolites. Current models on plant defense signaling networks in plant-herbivore interactions can now be expanded to include auxins as potentially important defense hormones.

## MATERIALS AND METHODS

### Plant Genotypes, Germination, and Planting Conditions

Wild-type *Nicotiana attenuata* plants of the 31st inbred generation derived from seeds collected at the Desert Inn Ranch in Utah in 1988 and all genetically engineered plant genotypes were germinated on Gamborg's B5 medium as described (Krügel et al., 2002). Nine to ten days later, seedlings were transferred to Teku pots (Pöppelmann) for 10 to 12 d before transferring them to 1-liter pots filled with either sand (to facilitate the harvesting of belowground tissues) or soil. All plants were grown at 45 to 55% relative humidity and 23 to 25°C during days and 19 to 23°C during nights under 16 h of light (6 AM–10 PM). Plants planted in soil were watered every day by a flood irrigation system. Plants planted in sand were watered twice a day. The characteristics of the transgenic plants used in this study are presented in Table I.

### Auxin and JA Measurements

Phytohormone measurements were conducted as described earlier (Machado et al., 2013, 2015). Briefly, plant tissues were harvested, flash frozen, and stored at  $-80^{\circ}\text{C}$ . After grinding, 100 mg of plant tissue per sample was extracted with 1 mL ethyl acetate:formic acid (99.5:0.5 v/v) containing the following phytohormone standards: 40 ng of 9,10- $\text{D}_2$ -9,10-dihydrojasmonic acid (JA), 8 ng of jasmonic acid- $[\text{13C}_6]$  Ile (JA-Ile), and 20 ng of  $\text{D}_5$ -indole-3-acetic acid (IAA). All samples were then vortexed for 10 min and centrifuged at 14,000 rpm for 20 min at  $4^{\circ}\text{C}$ . Supernatants were evaporated to dryness in a centrifugal vacuum concentrator (Eppendorf 5301) at room temperature. The remaining pellets were resuspended in 50  $\mu\text{L}$  methanol:water (70:30) and dissolved using an ultrasonic cleaner (Branson 1210; Branson Ultrasonics) for 5 min. Samples were then analyzed using liquid chromatography (Agilent 1260 Infinity Quaternary LC system; Agilent Technologies) coupled to a triple quadrupole mass spectrometer (API 5000 LC/MS/MS; Applied Biosystems).

### IAA Levels in Herbivore-Attacked Plants

IAA levels were determined in local, treated leaves of plant subjected to real or simulated *Manduca sexta* attack. Plants were infested by placing three first-instar larvae on one fully developed rosette leaf ( $n = 3$ ). Caterpillars were removed, and attacked leaves were harvested. *M. sexta* attack was simulated by rolling a pattern wheel over the leaves on each side of the midvein. Three fully developed rosette leaves were wounded and the resulting wounds were immediately treated with either 1:5 (v/v) water-diluted *M. sexta* oral secretions (W+OS), with pure water (W+W), or with fatty acid-amino acid conjugates (FACs; *N*-linolenoyl-Glu) as described (Xu et al., 2015; Machado et al., 2013). Intact plants were used as controls ( $n = 5$ ).

### *M. sexta*-Induced Auxin Levels in Different Plant Tissues

Forty-day-old elongating plants were subjected to simulated *M. sexta* attack as described above. Five, 10, 30, 60, and 120 min after elicitation, treated leaves and their untreated petioles, as well as stems, systemic leaves (young leaves directly

above treated leaves), and main and lateral roots were harvested. The same plant tissues were collected from untreated control plants at each time point ( $n = 5$ ).

### *M. sexta*-Induced Auxin Levels at Different Developmental Stages

IAA levels were measured at three developmental stages: early rosette (32 d after germination), elongating (39 d after germination), and flowering (46 d after germination). Tissues were harvested at three time points after elicitation as described above: 0.5, 1, and 3 h ( $n = 5$ ).

### Identification and Expression Profiling of YUCCA-Like Genes

YUCCA genes encode for flavin monooxygenase-like proteins that convert indole-3-pyruvic acid into IAA, a catalytic reaction that is currently seen as the limiting step of IAA biosynthesis (Mashiguchi et al., 2011). To identify YUCCA-like genes in *N. attenuata*, we searched the Arabidopsis (*Arabidopsis thaliana*) YUCCA2 gene sequence (NCBI accession no. NM\_117399.3) in the *N. attenuata* draft genome (Ling et al., 2015) using BLAST (E-value  $< 1\text{e-}10$ ; bit score  $> 200$ ) and reconstructed the phylogenetic tree of the gene family. We then designed specific primers (Supplemental Table S1) for each gene using Primique (Fredslund and Lange, 2007) and profiled gene expression patterns upon simulated *M. sexta* attack by quantitative real-time PCR ( $n = 3$ ). Total RNA was extracted by the Trizol method, followed by DNase-I treatment (Fermentas) according to the manufacturer's instructions. Five micrograms of total RNA was reverse-transcribed using oligo(dT)<sub>18</sub> and the SuperScript-II reverse transcriptase kit (Invitrogen). The obtained cDNA was used for gene expression profiling with SYBR Green I following the manufacturer's protocol, and the  $\Delta\text{Ct}$  method was used for transcript evaluation. The housekeeping gene actin was used as reference. Gene expression levels were determined 3, 5, and 60 min after elicitation.

### Characterization of the YUCCA-Like Gene Family

The YUCCA-like gene family sequences were aligned by ClustalW (Thompson et al., 1994) in BioEdit (Hall, 1999) and the occurrence of the already described conserved amino acid motifs characteristic of the flavin monooxygenase gene family was determined (Expósito-Rodríguez et al., 2011; Expósito-Rodríguez et al., 2007).

### OS-Induced Auxin and JA Kinetics

Rosette leaves of wild-type plants were subjected to simulated *M. sexta* attack (W+OS) as described and harvested 5, 45, and 90 min after elicitation ( $n = 5$ ). Phytohormone measurements were carried out as described.

### *M. sexta*-Induced Auxin Levels in JA and Signaling Impaired Genotypes

Three rosette leaves of rosette-stage plant genotypes impaired in salicylic acid-induced and wound-induced mitogen-activated protein kinases (irSIPK and irWIPK, respectively), JA biosynthesis (irGLA, irAOS, irAOC, and irOPR3), JA-Ile biosynthesis (irJAR4/6), jasmonate perception (irCOI1), wild type, and empty vector were subjected to *M. sexta* simulated attack as described. Forty-five minutes after elicitation, the leaves were harvested and analyzed for IAA, JA, and JA-Ile ( $n = 5$ ). These transgenic plant genotypes were selected as they are impaired at different layers of the jasmonate signaling cascade: early regulatory elements (irSIPK and irWIPK), JA biosynthesis (irGLA, irAOS, irAOC, and irOPR3), hormone activation (irJAR4/6), and hormone perception (irCOI1), and their main characteristics are listed in Table I.

### Stem Anthocyanin Quantifications

To determine the role of IAA in *M. sexta* induced stem anthocyanin accumulation, we carried out three experiments. First, we measured anthocyanins in the stem of plants whose rosette leaves were either left intact (Control), wounded and treated with water (W+W), wounded and treated with *M. sexta* oral secretions (W+OS), subjected to real, continuous *M. sexta* attack (*M. sexta*), treated with the natural auxin IAA (IAA), MeJA, or with both IAA and MeJA

(IAA+MeJA) dissolved in lanoline paste ( $n = 5$ ). Simulated *M. sexta* attack treatments were carried out as described above. Hormonal treatments were carried out as described below. In the second experiment, we measured stem anthocyanins in plants whose petioles were treated (petiole pretreatment) with the IAA biosynthesis inhibitor  $\tau$ -Kyn (He et al., 2011), the IAA transport inhibitor TIBA (Hertel et al., 1983; Goldsmith, 1982; Rubery, 1979), or with the natural auxin IAA prior to eliciting the plants by simulated *M. sexta* attack (W+OS) ( $n = 12$ ). One hour prior to the simulated *M. sexta* attack treatments,  $\sim 2 \mu\text{g}$  of  $\tau$ -Kyn, TIBA, or IAA, or  $150 \mu\text{g}$  MeJA dissolved in lanoline paste were applied to the petioles. Applied doses were selected according to previous studies ( $n = 12$ ; Baldwin, 1989; Morris et al., 1973; Kang et al., 2006; He et al., 2011). In a third experiment, we measured changes in stem anthocyanin levels upon simulated *M. sexta* herbivory in jasmonate-deficient irAOC and empty vector controls ( $n = 10$ ). Simulated and real *M. sexta* attack treatments were carried out as described. For all the experiments, the stems were harvested 5 d after treatments, and the anthocyanin content of the outer layer (epidermis, cortex, phloem, and cambium) was determined 5 cm above the shoot-root junction as described (Stephuhn et al., 2010).

### Stem Secondary Metabolite Quantifications

To further explore the regulatory role of IAA in secondary metabolite production, we induced the leaves of *N. attenuata* plants using real and simulated *M. sexta* attack treatments. Plants were either pretreated with IAA in lanolin paste or with pure lanolin as controls as described above. Petiole pretreatments with IAA were carried out 1 h prior to induction. Five days after induction, the stems were harvested and secondary metabolites were measured as described ( $n = 5$ ; Gaquerel et al., 2010; Ferrieri et al., 2015).

### Statistics

All data were analyzed by ANOVA using Sigma Plot 12.0 (Systat Software). Normality and equality of variance were verified using Shapiro-Wilk and Levene's tests, respectively. Holm-Sidak post hoc tests were used for multiple comparisons. Data sets from experiments that did not fulfill the assumptions for ANOVA were natural log-, root square-, or rank-transformed before analysis. Correlation between jasmonate and IAA levels, and stem coloration index and stem anthocyanin content, were evaluated by Pearson product moment test.

### Accession Numbers

Sequence data from this article can be found in the GenBank/EMBL data libraries under accession numbers BankIt1947548 Seq1 KX768736, BankIt1947548 Seq2 KX768737, BankIt1947548 Seq3 KX768738, BankIt1947548 Seq4 KX768739, BankIt1947548 Seq5 KX768740, BankIt1947548 Seq6 KX768741, BankIt1947548 Seq7 KX768742, BankIt1947548 Seq8 KX768743, and BankIt1947548 Seq9 KX768744.

### Supplemental Data

The following supplemental materials are available.

**Supplemental Figure S1.** IAA is induced locally in response to simulated *M. sexta* herbivory independently of time of day.

**Supplemental Figure S2.** The *N. attenuata* genome contains nine YUCCA-like genes.

**Supplemental Figure S3.** Gene expression patterns of YUCCA-like genes upon simulated *M. sexta* attack.

**Supplemental Figure S4.** Jasmonate signaling is not required for the *M. sexta*-induced accumulation of IAA.

**Supplemental Table S1.** Sequence of primers used for quantitative PCR analysis.

### ACKNOWLEDGMENTS

All experimental work of this study was supported by the Max Planck Society. We thank the members of the Department of Molecular Ecology and the glasshouse team of the MPI-CE for their help. We also thank Mareike Schirmer and

Mareike Schmidt for technical support and Wenwu Zhou, Martin Schäfer, and Michael Reichelt for their valuable help with the auxin measurements.

Received July 9, 2016; accepted July 28, 2016; published August 2, 2016.

### LITERATURE CITED

- Agtuca B, Rieger E, Hilger K, Song L, Am Robert C, Erb M, Karve A, Ferrieri RA** (2014) Carbon-11 reveals opposing roles of auxin and salicylic acid in regulating leaf physiology, leaf metabolism, and resource allocation patterns that impact root growth in *Zea mays*. *J Plant Growth Regul* **33**: 328–339
- Baldwin IT** (1989) Mechanism of damage-induced alkaloid production in wild tobacco. *J Chem Ecol* **15**: 1661–1680
- Baldwin IT, Zhang Z-P, Diab N, Ohnmeiss TE, McCloud ES, Lynds GY, Schmelz EA** (1997) Quantification, correlations and manipulations of wound-induced changes in jasmonic acid and nicotine in *Nicotiana sylvestris*. *Planta* **201**: 397–404
- Bartlett L, Connor EF** (2014) Exogenous phytohormones and the induction of plant galls by insects. *Arthropod-Plant Interact* **8**: 339–348
- Bhalerao RP, Eklöf J, Ljung K, Marchant A, Bennett M, Sandberg G** (2002) Shoot-derived auxin is essential for early lateral root emergence in Arabidopsis seedlings. *Plant J* **29**: 325–332
- Bonaventure G, Schuck S, Baldwin IT** (2011) Revealing complexity and specificity in the activation of lipase-mediated oxylipin biosynthesis: a specific role of the *Nicotiana attenuata* GLA1 lipase in the activation of jasmonic acid biosynthesis in leaves and roots. *Plant Cell Environ* **34**: 1507–1520
- Borevitz JO, Xia Y, Blount J, Dixon RA, Lamb C** (2000) Activation tagging identifies a conserved MYB regulator of phenylpropanoid biosynthesis. *Plant Cell* **12**: 2383–2394
- Chen Q, Sun J, Zhai Q, Zhou W, Qi L, Xu L, Wang B, Chen R, Jiang H, Qi J, et al** (2011) The basic helix-loop-helix transcription factor MYC2 directly represses PLETHORA expression during jasmonate-mediated modulation of the root stem cell niche in Arabidopsis. *Plant Cell* **23**: 3335–3352
- Connor EF, Bartlett L, O'Toole S, Byrd S, Biskar K, Orozco J** (2012) The mechanism of gall induction makes galls red. *Arthropod-Plant Interact* **6**: 489–495
- Dafoe NJ, Thomas JD, Shirk PD, Legaspi ME, Vaughan MM, Huffaker A, Teal PE, Schmelz EA** (2013) European corn borer (*Ostrinia nubilalis*) induced responses enhance susceptibility in maize. *PLoS One* **8**: e73394
- De Geyter N, Gholami A, Goormachtig S, Goossens A** (2012) Transcriptional machineries in jasmonate-elicited plant secondary metabolism. *Trends Plant Sci* **17**: 349–359
- DeWald DB, Sadka A, Mullet JE** (1994) Sucrose modulation of soybean Vsp gene expression is inhibited by auxin. *Plant Physiol* **104**: 439–444
- Diezel C, Allmann S, Baldwin IT** (2011a) Mechanisms of optimal defense patterns in *Nicotiana attenuata*: flowering attenuates herbivory-elicited ethylene and jasmonate signaling. *J Integr Plant Biol* **53**: 971–983
- Diezel C, Kessler D, Baldwin IT** (2011b) Pithy protection: *Nicotiana attenuata*'s jasmonic acid-mediated defenses are required to resist stem-boring weevil larvae. *Plant Physiol* **155**: 1936–1946
- Dorchin, N., Hoffmann, J.H., Stirk, W.A., Novák, O., Strnad, M., van Staden, J.** (2009) Sexually dimorphic gall structures correspond to differential phytohormone contents in male and female wasp larvae. *Physiol Entomol* **34**: 359–369
- Erb M, Meldau S, Howe GA** (2012) Role of phytohormones in insect-specific plant reactions. *Trends Plant Sci* **17**: 250–259
- Expósito-Rodríguez M, Borges AA, Borges-Pérez A, Hernández M, Pérez JA** (2007) Cloning and biochemical characterization of ToFZY, a tomato gene encoding a flavin monooxygenase involved in a tryptophan-dependent auxin biosynthesis pathway. *J Plant Growth Regul* **26**: 329–340
- Expósito-Rodríguez M, Borges AA, Borges-Pérez A, Pérez JA** (2011) Gene structure and spatiotemporal expression profile of tomato genes encoding YUCCA-like flavin monooxygenases: the ToFZY gene family. *Plant Physiol Biochem* **49**: 782–791
- Ferrieri AP, Arce CC, Machado RAR, Meza-Canales ID, Lima E, Baldwin IT, Erb M** (2015) A *Nicotiana attenuata* cell wall invertase inhibitor (NaCWII) reduces growth and increases secondary metabolite biosynthesis in herbivore-attacked plants. *New Phytol* **208**: 519–530

- Fredslund J, Lange M** (2007) Primique: automatic design of specific PCR primers for each sequence in a family. *BMC Bioinformatics* **8**: 369
- Friml J** (2003) Auxin transport - shaping the plant. *Curr Opin Plant Biol* **6**: 7–12
- Gaquerel E, Heiling S, Schoettner M, Zurek G, Baldwin IT** (2010) Development and validation of a liquid chromatography-electrospray ionization-time-of-flight mass spectrometry method for induced changes in *Nicotiana attenuata* leaves during simulated herbivory. *J Agric Food Chem* **58**: 9418–9427
- Geldner N, Friml J, Stierhof Y-D, Jürgens G, Palme K** (2001) Auxin transport inhibitors block PIN1 cycling and vesicle trafficking. *Nature* **413**: 425–428
- Glick BR** (2015). *Beneficial Plant-Bacterial Interactions*. Springer, Cham, Switzerland
- Goldsmith MHM** (1982) A saturable site responsible for polar transport of indole-3-acetic acid in sections of maize coleoptiles. *Planta* **155**: 68–75
- Guiscafrearrillaga J** (1949) Formation of galls in stems and leaves of sugar cane in response to injections of growth-regulating substances. *Phytopathology* **39**: 489–493
- Halitschke R, Gase K, Hui D, Schmidt DD, Baldwin IT** (2003) Molecular interactions between the specialist herbivore *Manduca sexta* (lepidoptera, sphingidae) and its natural host *Nicotiana attenuata*. VI. Microarray analysis reveals that most herbivore-specific transcriptional changes are mediated by fatty acid-amino acid conjugates. *Plant Physiol* **131**: 1894–1902
- Hall TA** (1999) BioEdit: a user-friendly biological sequence alignment editor and analysis program for Windows 95/98/NT. *Nucleic Acids Symp Ser* (41): 95–98
- Hammer KC, Kraus EJ** (1937) Histological reactions of bean plants to growth promoting substances. *Bot Gaz* **98**: 735–807
- He W, Brumos J, Li H, Ji Y, Ke M, Gong X, Zeng Q, Li W, Zhang X, An F, et al** (2011) A small-molecule screen identifies L-kynurenine as a competitive inhibitor of TAA1/TAR activity in ethylene-directed auxin biosynthesis and root growth in Arabidopsis. *Plant Cell* **23**: 3944–3960
- Heiling S, Schuman MC, Schoettner M, Mukerjee P, Berger B, Schneider B, Jassbi AR, Baldwin IT** (2010) Jasmonate and ppHsystemin regulate key malonylation steps in the biosynthesis of 17-hydroxygeranylinalool diterpene glycosides, an abundant and effective direct defense against herbivores in *Nicotiana attenuata*. *Plant Cell* **22**: 273–292
- Hertel R, Lomax TL, Briggs WR** (1983) Auxin transport in membrane vesicles from *Cucurbita pepo* L. *Planta* **157**: 193–201
- Hou X, Lee LYC, Xia K, Yan Y, Yu H** (2010) DELLAs modulate jasmonate signaling via competitive binding to JAZs. *Dev Cell* **19**: 884–894
- Howe GA, Jander G** (2008) Plant immunity to insect herbivores. *Annu Rev Plant Biol* **59**: 41–66
- Jimenez-Aleman GH, Machado RAR, Göröls H, Baldwin IT, Boland W** (2015) Synthesis, structural characterization and biological activity of two diastereomeric JA-Ile macrolactones. *Org Biomol Chem* **13**: 5885–5893
- Jin X, Zimmermann J, Polle A, Fischer U** (2015) Auxin is a long-range signal that acts independently of ethylene signaling on leaf abscission in *Populus*. *Front Plant Sci* **6**: 634
- Kallenbach M, Bonaventure G, Gilardoni PA, Wissgott A, Baldwin IT** (2012) Empoasca leafhoppers attack wild tobacco plants in a jasmonate-dependent manner and identify jasmonate mutants in natural populations. *Proc Natl Acad Sci USA* **109**: E1548–E1557
- Kang J-H, Wang L, Giri A, Baldwin IT** (2006) Silencing threonine deaminase and JAR4 in *Nicotiana attenuata* impairs jasmonic acid-isoleucine-mediated defenses against *Manduca sexta*. *Plant Cell* **18**: 3303–3320
- Kernan A, Thornburg RW** (1989) Auxin levels regulate the expression of a wound-inducible proteinase inhibitor II-chloramphenicol acetyl transferase gene fusion in vitro and in vivo. *Plant Physiol* **91**: 73–78
- Koo AJK, Gao X, Jones AD, Howe GA** (2009) A rapid wound signal activates the systemic synthesis of bioactive jasmonates in Arabidopsis. *Plant J* **59**: 974–986
- Kramer EM, Rutschow HL, Mabie SS** (2011) AuxV: a database of auxin transport velocities. *Trends Plant Sci* **16**: 461–463
- Kroes A, van Loon JJA, Dicke M** (2015) Density-dependent interference of aphids with caterpillar-induced defenses in Arabidopsis: Involvement of phytohormones and transcription factors. *Plant Cell Physiol* **56**: 98–106
- Krügel T, Lim M, Gase K, Halitschke R, Baldwin IT** (2002) Agrobacterium-mediated transformation of *Nicotiana attenuata*, a model ecological expression system. *Chemoecology* **12**: 177–183
- Kurepin LV, Park JM, Lazarovits G, Bernards MA** (2015) Burkholderia phytofirmans-induced shoot and root growth promotion is associated with endogenous changes in plant growth hormone levels. *Plant Growth Regul* **75**: 199–207
- Lambrech M, Okon, Y., Broek, A.V., Vanderleyden, J.** (2000). Indole-3-acetic acid: a reciprocal signalling molecule in bacteria-plant interactions. *Evolution* **54**: 59.
- Lee G, Joo Y, Diezel C, Lee EJ, Baldwin IT, Kim SG** (2016) Trichobaris weevils distinguish amongst toxic host plants by sensing volatiles that do not affect larval performance. *Mol Ecol* **25**: 3509–3519
- Lewis DR, Ramirez MV, Miller ND, Vallabhaneni P, Ray WK, Helm RF, Winkel BSJ, Muday GK** (2011) Auxin and ethylene induce flavonol accumulation through distinct transcriptional networks. *Plant Physiol* **156**: 144–164
- Li R, Zhang J, Li J, Zhou G, Wang Q, Bian W, Erb M, Lou Y** (2015) Prioritizing plant defence over growth through WRKY regulation facilitates infestation by non-target herbivores. *eLife* **4**: e04805
- Ling Z, Zhou W, Baldwin IT, Xu S** (2015) Insect herbivory elicits genome-wide alternative splicing responses in *Nicotiana attenuata*. *Plant J* **84**: 228–243
- Liu Y, Ahn J-E, Datta S, Salzman RA, Moon J, Huyghues-Despointes B, Pittendrigh B, Murdock LL, Koiwa H, Zhu-Salzman K** (2005) Arabidopsis vegetative storage protein is an anti-insect acid phosphatase. *Plant Physiol* **139**: 1545–1556
- Lulu T, Park S-Y, Ibrahim R, Paek K-Y** (2015) Production of biomass and bioactive compounds from adventitious roots by optimization of culturing conditions of *Eurycoma longifolia* in balloon-type bubble bioreactor system. *J Biosci Bioeng* **119**: 712–717
- Maag D, Köhler A, Robert CAM, Frey M, Wolfender JL, Turlings TCJ, Glauser G, Erb M** (2016) Highly localised and persistent induction of *Bx1*-dependent herbivore resistance factors in maize. *Plant J* (in press)
- Machado RAR, Arce CC, Ferrieri AP, Baldwin IT, Erb M** (2015) Jasmonate-dependent depletion of soluble sugars compromises plant resistance to *Manduca sexta*. *New Phytol* **207**: 91–105
- Machado RAR, Ferrieri AP, Robert CA, Glauser G, Kallenbach M, Baldwin IT, Erb M** (2013) Leaf-herbivore attack reduces carbon reserves and regrowth from the roots via jasmonate and auxin signaling. *New Phytol* **200**: 1234–1246
- Machado RAR, McClure M, Hervé MR, Baldwin IT, Erb M** (2016) Benefits of jasmonate-dependent defenses against vertebrate herbivores in nature. *eLife* **5**: e13720
- Mahdieh M, Noori M, Hoseinkhani S** (2015) Studies of in vitro adventitious root induction and flavonoid profiles in *Rumex crispus*. *Adv Life Sci* **5**: 53–57
- Mano Y, Nemoto K** (2012) The pathway of auxin biosynthesis in plants. *J Exp Bot* **63**: 2853–2872
- Mapes CC, Davies PJ** (2001a) Cytokinins in the ball gall of *Solidago altissima* and in the gall forming larvae of Eurosta solidaginis. *New Phytol* **151**: 203–212
- Mapes CC, Davies PJ** (2001b) Indole-3-acetic acid and ball gall development on *Solidago altissima*. *New Phytol* **151**: 195–202
- Mashiguchi K, Tanaka K, Sakai T, Sugawara S, Kawaide H, Natsume M, Hanada A, Yaeno T, Shirasu K, Yao H, et al** (2011) The main auxin biosynthesis pathway in Arabidopsis. *Proc Natl Acad Sci USA* **108**: 18512–18517
- Meldau S, Wu J, Baldwin IT** (2009) Silencing two herbivory-activated MAP kinases, SIPK and WIPK, does not increase *Nicotiana attenuata*'s susceptibility to herbivores in the glasshouse and in nature. *New Phytol* **181**: 161–173
- Morris DA, Kadir GO, Barry AJ** (1973) Auxin transport in intact pea seedlings (*Pisum sativum* L.): The inhibition of transport by 2,3,5-triiodobenzoic acid. *Planta* **110**: 173–182
- Mousavi SAR, Chauvin A, Pascaud F, Kellenberger S, Farmer EE** (2013) GLUTAMATE RECEPTOR-LIKE genes mediate leaf-to-leaf wound signalling. *Nature* **500**: 422–426
- Onkokesung N, Gális I, von Dahl CC, Matsuoka K, Saluz H-P, Baldwin IT** (2010) Jasmonic acid and ethylene modulate local responses to wounding and simulated herbivory in *Nicotiana attenuata* leaves. *Plant Physiol* **153**: 785–798
- Onkokesung N, Gaquerel E, Kotkar H, Kaur H, Baldwin IT, Galis I** (2012) MYB8 controls inducible phenolamide levels by activating three novel hydroxycinnamoyl-coenzyme A:polyamine transferases in *Nicotiana attenuata*. *Plant Physiol* **158**: 389–407

- Paschold A, Halitschke R, Baldwin IT** (2007) Co(i)-ordinating defenses: NaCOI1 mediates herbivore-induced resistance in *Nicotiana attenuata* and reveals the role of herbivore movement in avoiding defenses. *Plant J* **51**: 79–91
- Pasqua G, Monacelli B, Mulinacci N, Rinaldi S, Giaccherini C, Innocenti M, Vinceri FF** (2005) The effect of growth regulators and sucrose on anthocyanin production in *Camptotheca acuminata* cell cultures. *Plant Physiol Biochem* **43**: 293–298
- Qi T, Song S, Ren Q, Wu D, Huang H, Chen Y, Fan M, Peng W, Ren C, Xie D** (2011) The Jasmonate-ZIM-domain proteins interact with the WD-Repeat/bHLH/MYB complexes to regulate Jasmonate-mediated anthocyanin accumulation and trichome initiation in *Arabidopsis thaliana*. *Plant Cell* **23**: 1795–1814
- Reed RC, Brady SR, Muday GK** (1998) Inhibition of auxin movement from the shoot into the root inhibits lateral root development in *Arabidopsis*. *Plant Physiol* **118**: 1369–1378
- Rubery PH** (1979) The effects of 2,4-dinitrophenol and chemical modifying reagents on auxin transport by suspension-cultured crown gall cells. *Planta* **144**: 173–178
- Sassi M, Lu Y, Zhang Y, Wang J, Dhonukshe P, Blilou I, Dai M, Li J, Gong X, Jaillais Y, et al** (2012) COP1 mediates the coordination of root and shoot growth by light through modulation of PIN1- and PIN2-dependent auxin transport in *Arabidopsis*. *Development* **139**: 3402–3412
- Schäfer M, Brütting C, Gase K, Reichelt M, Baldwin I, Meldau S** (2013) 'Real time' genetic manipulation: a new tool for ecological field studies. *Plant J* **76**: 506–518
- Schäfer M, Meza-Canales, I.D., Brütting, C., Baldwin, I.T., Meldau, S.** (2015). Cytokinin concentrations and CHASE-DOMAIN CONTAINING HIS KINASE 2 (NaCHK2)- and NaCHK3-mediated perception modulate herbivory-induced defense signaling and defenses in *Nicotiana attenuata*. *New Phytol* **207**: 645–658
- Schäller G** (1968) Biochemische Analyse des Aphidenspeichels und seine Bedeutung für die Gallenbildung. *Zool Jb Physiol* **74**: 54–87
- Schmelz EA, Engelberth J, Alborn HT, O'Donnell P, Sammons M, Toshima H, Tumlinson III JH** (2003) Simultaneous analysis of phytohormones, phytotoxins, and volatile organic compounds in plants. *Proc Natl Acad Sci USA* **100**: 10552–10557
- Shi Q, Li C, Zhang F** (2006) Nicotine synthesis in *Nicotiana tabacum* L. induced by mechanical wounding is regulated by auxin. *J Exp Bot* **57**: 2899–2907
- Shin DH, Cho M, Choi MG, Das PK, Lee S-K, Choi S-B, Park Y-I** (2015) Identification of genes that may regulate the expression of the transcription factor production of anthocyanin pigment 1 (PAP1)/MYB75 involved in *Arabidopsis* anthocyanin biosynthesis. *Plant Cell Rep* **34**: 805–815
- Song Y** (2014) Insight into the mode of action of 2,4-dichlorophenoxyacetic acid (2,4-D) as an herbicide. *J Integr Plant Biol* **56**: 106–113
- Steppuhn A, Gaquerel E, Baldwin IT** (2010) The two  $\alpha$ -dox genes of *Nicotiana attenuata*: overlapping but distinct functions in development and stress responses. *BMC Plant Biol* **10**: 171
- Stitz M, Gase K, Baldwin IT, Gaquerel E** (2011) Ectopic expression of AtJMT in *Nicotiana attenuata*: creating a metabolic sink has tissue-specific consequences for the jasmonate metabolic network and silences downstream gene expression. *Plant Physiol* **157**: 341–354
- Straka JR, Hayward AR, Emery RN** (2010) Gall-inducing *Pachypsylla celtidis* (Psyllidae) infiltrate hackberry trees with high concentrations of phytohormones. *J Plant Interact* **5**: 197–203
- Tanaka Y, Okada K, Asami T, Suzuki Y** (2013) Phytohormones and willow gall induction by a gall-inducing sawfly. *Biosci Biotechnol Biochem* **77**: 1942–1948
- Tanaka Y, Uritani I** (1979) Polar transport and content of indole-3-acetic acid in wounded sweet potato root tissues. *Plant Cell Physiol* **20**: 1087–1095
- Thaler JS, Bostock RM** (2004) Interactions between abscisic-acid-mediated responses and plant resistance to pathogens and insects. *Ecology* **85**: 48–58
- Thompson JD, Higgins DG, Gibson TJ** (1994) CLUSTAL W: improving the sensitivity of progressive multiple sequence alignment through sequence weighting, position-specific gap penalties and weight matrix choice. *Nucleic Acids Res* **22**: 4673–4680
- Thornburg RW, Li X** (1991) Wounding *Nicotiana tabacum* leaves causes a decline in endogenous indole-3-acetic acid. *Plant Physiol* **96**: 802–805
- Tian Q, Chen F, Liu J, Zhang F, Mi G** (2008) Inhibition of maize root growth by high nitrate supply is correlated with reduced IAA levels in roots. *J Plant Physiol* **165**: 942–951
- Tooker JF, de Moraes CM** (2011a) Feeding by a gall-inducing caterpillar species alters levels of indole-3-acetic and abscisic acid in *Solidago altissima* (Asteraceae) stems. *Arthropod-Plant Interact* **5**: 115–124
- Tooker JF, de Moraes CM** (2011b) Feeding by Hessian fly (*Mayetiola destructor* [Say]) larvae on wheat increases levels of fatty acids and indole-3-acetic acid but not hormones involved in plant-defense signaling. *J Plant Growth Regul* **30**: 158–165
- VanDoorn A, Bonaventure G, Schmidt DD, Baldwin IT** (2011) Regulation of jasmonate metabolism and activation of systemic signaling in *Solanum nigrum*: COI1 and JAR4 play overlapping yet distinct roles. *New Phytol* **190**: 640–652
- van Noorden GE, Ross JJ, Reid JB, Rolfe BG, Mathesius U** (2006) Defective long-distance auxin transport regulation in the *Medicago truncatula* super numeric nodules mutant. *Plant Physiol* **140**: 1494–1506
- Von Dahl CC, Baldwin IT** (2004) Methyl jasmonate and cis-jasmonate do not dispose of the herbivore-induced jasmonate burst in *Nicotiana attenuata*. *Physiol Plant* **120**: 474–481
- von Dahl CC, Winz RA, Halitschke R, Kühnemann F, Gase K, Baldwin IT** (2007) Tuning the herbivore-induced ethylene burst: the role of transcript accumulation and ethylene perception in *Nicotiana attenuata*. *Plant J* **51**: 293–307
- Wang L, Allmann S, Wu J, Baldwin IT** (2008) Comparisons of LIPOXY-GENASE3- and JASMONATE-RESISTANT4/6-silenced plants reveal that jasmonic acid and jasmonic acid-amino acid conjugates play different roles in herbivore resistance of *Nicotiana attenuata*. *Plant Physiol* **146**: 904–915
- Wasternack C, Hause B** (2013) Jasmonates: biosynthesis, perception, signal transduction and action in plant stress response, growth and development. An update to the 2007 review in *Annals of Botany*. *Ann Bot (Lond)* **111**: 1021–1058
- Weinhold A, Kallenbach M, Baldwin IT** (2013) Progressive 35S promoter methylation increases rapidly during vegetative development in transgenic *Nicotiana attenuata* plants. *BMC Plant Biol* **13**: 99
- Winz RA, Baldwin IT** (2001) Molecular interactions between the specialist herbivore *Manduca sexta* (Lepidoptera, Sphingidae) and its natural host *Nicotiana attenuata*. IV. Insect-Induced ethylene reduces jasmonate-induced nicotine accumulation by regulating putrescine N-methyltransferase transcripts. *Plant Physiol* **125**: 2189–2202
- Woldemariam MG, Onkokesung N, Baldwin IT, Galis I** (2012) Jasmonoyl-L-isoleucine hydrolase 1 (JIH1) regulates jasmonoyl-L-isoleucine levels and attenuates plant defenses against herbivores. *Plant J* **72**: 758–767
- Wu J, Baldwin IT** (2009) Herbivory-induced signalling in plants: perception and action. *Plant Cell Environ* **32**: 1161–1174
- Xin Z, Yu Z, Erb M, Turlings TCJ, Wang B, Qi J, Liu S, Lou Y** (2012) The broad-leaf herbicide 2,4-dichlorophenoxyacetic acid turns rice into a living trap for a major insect pest and a parasitic wasp. *New Phytol* **194**: 498–510
- Xu S, Zhou W, Pottinger S, Baldwin IT** (2015) Herbivore associated elicitor-induced defences are highly specific among closely related *Nicotiana* species. *BMC Plant Biol* **15**: 2
- Yamaguchi H, Tanaka H, Hasegawa M, Tokuda M, Asami T, Suzuki Y** (2012) Phytohormones and willow gall induction by a gall-inducing sawfly. *New Phytol* **196**: 586–595
- Yang D-L, Yao J, Mei C-S, Tong X-H, Zeng L-J, Li Q, Xiao L-T, Sun TP, Li J, Deng X-W, et al** (2012) Plant hormone jasmonate prioritizes defense over growth by interfering with gibberellin signaling cascade. *Proc Natl Acad Sci USA* **109**: E1192–E1200
- Yang F, Song Y, Yang H, Liu Z, Zhu G, Yang Y** (2014) An auxin-responsive endogenous peptide regulates root development in *Arabidopsis*. *J Integr Plant Biol* **56**: 635–647
- Zhang P-J, Li W-D, Huang F, Zhang J-M, Xu F-C, Lu Y-B** (2013) Feeding by whiteflies suppresses downstream jasmonic acid signaling by eliciting salicylic acid signaling. *J Chem Ecol* **39**: 612–619

Supplementary material

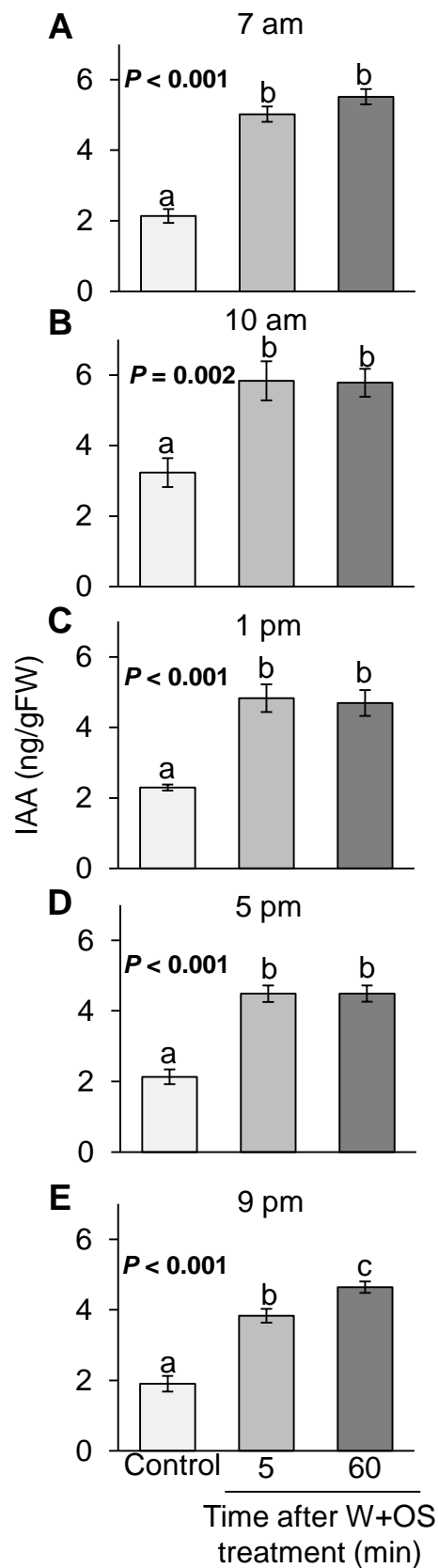


**Figure S1.** IAA is induced locally in response to simulated *M. sexta* herbivory independently of time of day. Average ( $\pm$ SE) IAA content in the leaves of plants that were subjected to simulated *M. sexta* attack at 7 am (a), 10 am (b), 1pm (c), 5pm (d) or 9pm (e) 5 and 60 minutes after treatments. Different letters indicate significant differences between treatments ( $P < 0.05$ ).

	<b>FAD-binding</b>	<b>Hallmark 1</b>	<b>NADH-binding</b>	<b>Hallmark 2</b>
<b>NaYUCCA-like 1</b>	GAGPSGLA	WLVVATGENAE	GCGNSGME	DSVVLATGYCSNVP
<b>NaYUCCA-like 2</b>	GAGPSGLA	WLVVATGENAE	GCGNSGME	DSVILATGYCSNVP
<b>NaYUCCA-like 3</b>	GAGPSGLA	WLVVATGENAE	GCGNSGME	DSVVLATGYCSNVP
<b>NaYUCCA-like 4</b>	GGGPSGLA	WLVVATGENAE	GCGNSGME	DSVVLATGYCSNVP
<b>NaYUCCA-like 5</b>	GAGPAGLA	FLVLASGENSE	GCGNSGME	DVIVFATGFKRTH
<b>NaYUCCA-like 6</b>	GAGPSGLA	WLVVATGENAE	GCGNSGME	DSIILATGYKSNVP
<b>NaYUCCA-like 7</b>	GGGPSGLA	WLVVATGENAE	GCGNSGME	DAIILATGYKSNVP
<b>NaYUCCA-like 8</b>	GAGPSGLA	WLVVATGENAE	GCGNSGME	DAIILATGYKSNVP
<b>NaYUCCA-like 9</b>	GAGPAGIA	FLVLASGENSE	GCGNSGME	DAMVFATGYKSTVT

**Figure S2.** *N. attenuata* genome contains nine *YUCCA*-like genes. Multiple alignment of four conserved amino acid motifs found in the ten-membered NaYUCCA-like gene family.

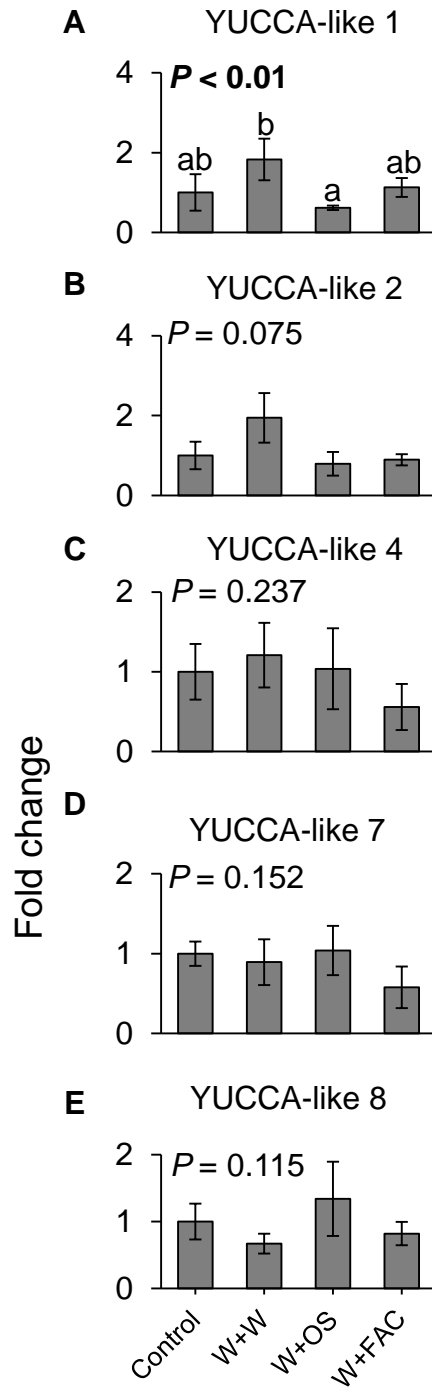


**Figure S3.** Gene expression patterns of YUCCA-like genes upon simulated *M. sexta* attack. Average ( $\pm$ SE) transcript abundance relative to control of YUCCA-like 1 (A), YUCCA-like 2 (B), YUCCA-like 4 (C), YUCCA-like 7 (D) and YUCCA-like 8 (E) genes followed simulated *M. sexta* attack (n=3). Different letters indicate significant differences between treatments ( $P < 0.05$ ).

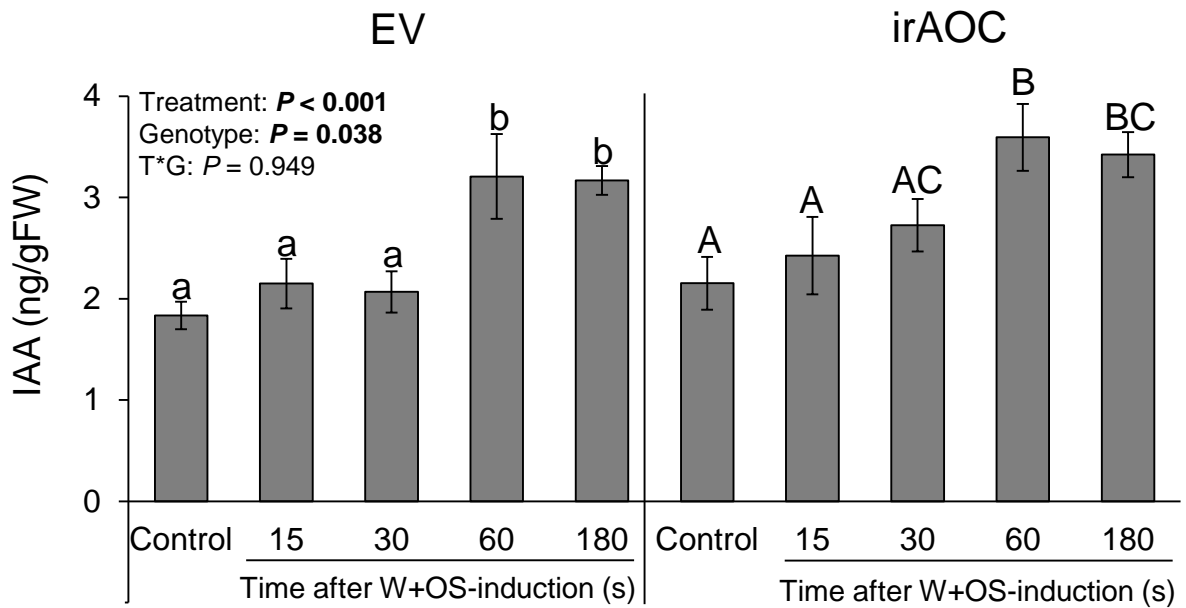


**Figure S4.** *Jasmonate signaling is not required for the *M. sexta*-induced accumulation of IAA.* Average ( $\pm$ SE) IAA levels in local, treated leaves of wild type plants (empty vector; EV) and jasmonate-deficient inverted repeat allene-oxide cyclase (irAOC) plants (n=5). Different letters indicate significant differences between treatments within each genotype ( $P < 0.05$ ). W+OS: wounded and *M. sexta* oral secretions-treated plants.